

# Application of ion beam to fabricate $\beta$ -FeSi<sub>2</sub> and to control its photoluminescence properties.

(イオンビームを利用した  $\beta$ -FeSi<sub>2</sub> 作製およびその発光特性制御)

氏名 ジュラブリョフ アレクセイ ヴァレリービッチ

## 1. Introduction.

Semiconducting silicides are extensively studied in the recent years because of their promising properties as Si-based electronic devices [1]. Among them, beta-iron disilicide,  $\beta$ -FeSi<sub>2</sub>, formed on a Si substrate, is known to exhibit photoluminescence (PL) peak at around 0.8 eV. However, substrate Si also has a luminescence peak at 0.80 eV, which nearly coincides with that of  $\beta$ -FeSi<sub>2</sub>, so that the origin of PL peak from  $\beta$ -FeSi<sub>2</sub> / Si is always point of issue. On the other hand, the ion beam sputter deposition (IBSD) method was successfully applied to fabrication of  $\beta$ -FeSi<sub>2</sub> film on Si substrate [2]. It is interest to see how the ion-induced processes in IBSD affect the PL properties. In this study, the fabrication process and PL properties of IBSD-grown  $\beta$ -FeSi<sub>2</sub> were investigated with reference to ion-induced effects.

## 2. Experimental.

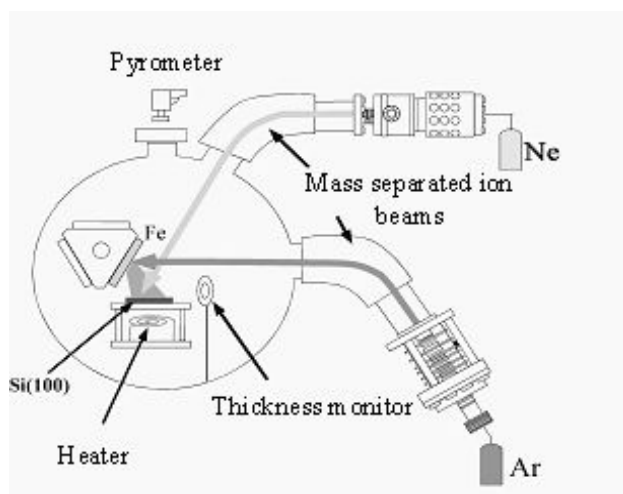


Fig. 1: Schematic diagram of IBSD device.

The  $\beta$ -FeSi<sub>2</sub> films were grown by the IBSD method. In Fig.1 the schematic diagram of IBSD device is shown. The typical deposition procedures are as follows: (1) ultrasonic cleaning of the Si samples in acetone, ethylene and water, before installing in a ultra-high vacuum ( $10^{-7}$  Pa) vessel, (2) sputter etching (SE) of the sample by Ne<sup>+</sup> ion beam (3 keV, 5  $\mu$ A, 20 min), annealing the sample for 1 hour at 973 K, and (3) sputter deposition of Fe target by Ar<sup>+</sup> ion beam (35 keV, 180  $\mu$ A, 60 min). In photoluminescence (PL) measurement, the samples were excited by 532 nm solid-state laser with an output power of 50-100 mW, and PL spectra were obtained in the temperature range of 10-300 K. Luminescence was analyzed in the wavelength region of 1100-1700 nm (0.73-1.12 eV). The scheme of  $\beta$ -FeSi<sub>2</sub> film growth process is shown in Fig. 2.

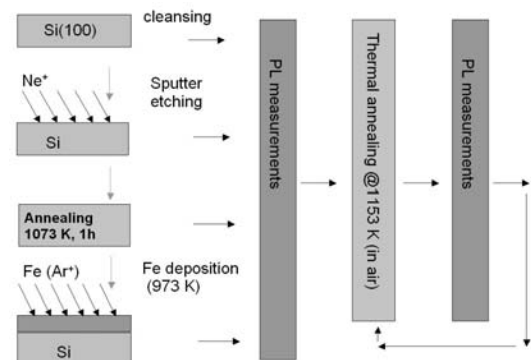


Fig. 2: Typical scheme of  $\beta$ -FeSi<sub>2</sub> film fabrication and characterization processes.

### 3. Photoluminescence (PL) characterization of $\beta$ -FeSi<sub>2</sub> prepared by ion beam sputter deposition (IBSD) method.

The various stages of IBSD method to prepare  $\beta$ -FeSi<sub>2</sub> film on Si substrate were characterized by PL measurement. It has been found that sputter etching of the substrate surface is essential to obtain highly oriented  $\beta$ -FeSi<sub>2</sub> film [3]. Fig. 3 shows the PL spectra of Si substrate, SE-treated Si and  $\beta$ -FeSi<sub>2</sub> film prepared on SE-treated Si substrate for CZ samples. All the samples shown in the figure were annealed in air at 1153 K for 20 hours and the spectra were measured at 34 K.

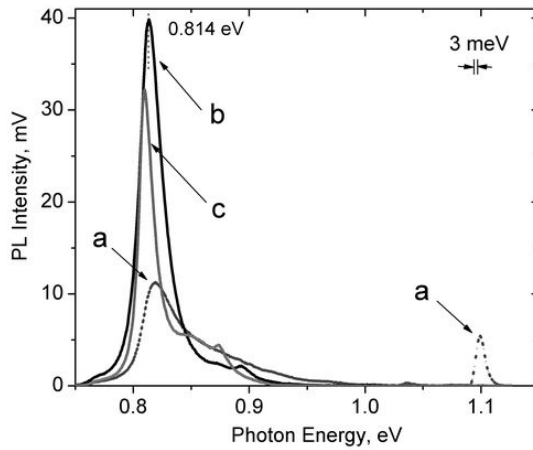


Fig. 3: PL spectra of (a) Si substrate, (b) SE-treated Si and (c)  $\beta$ -FeSi<sub>2</sub> film prepared on SE-treated Si substrate for CZ samples

It is clearly shown that the annealing drastically increased the PL intensity at around 0.81 eV. It should be noted that it was the samples that underwent Ne<sup>+</sup> sputter etching that showed most drastic increase of PL peak upon thermal annealing in air. For CZ sample, the largest intensity of 0.81 eV peak was obtained for SE-treated Si, followed by  $\beta$ -FeSi<sub>2</sub> formed on Si. Comparison between Si substrate (a) and SE-treated Si (b) indicates that annealing alone did not lead to such PL enhancement. It is thus clear that SE and thermal

annealing cooperatively enhanced the observed PL emission at 0.81 eV.

A previous study indicated that after high temperature annealing (above 1073 K) the morphology of  $\beta$ -FeSi<sub>2</sub> film changed to island structure [4], which fact indicates that some portion of the PL signal originated from the bulk of Si. Therefore, the PL signal from the annealed  $\beta$ -FeSi<sub>2</sub> formed on Si substrate may include contributions from both silicide and Si. From comparison of spectra b and c in Fig. 3, it is considered that contribution of Si substrate to the observed PL enhancement cannot be ignored.

Fig. 4 shows temperature dependence of the PL peak energy of the CZ samples used in this study, together with the data reported by Maeda et al. [5] and Binetti et al. [6].

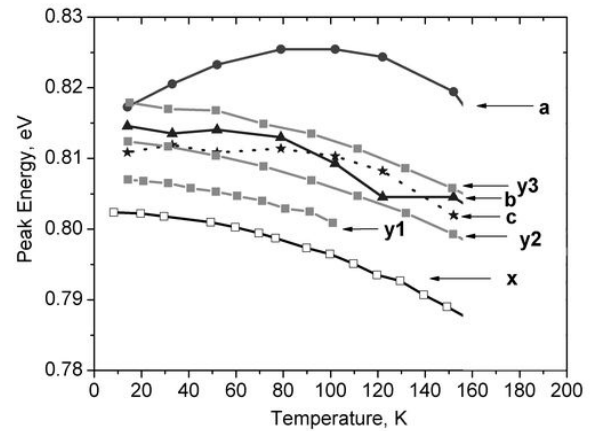


Fig. 4: Temperature dependence of the PL peak energy of the samples using CZ Si as a substrate; (a) CZ Si, (b) SE-treated CZ Si and (c)  $\beta$ -FeSi<sub>2</sub> film prepared on SE-treated CZ Si, together with literature data: (x) Maeda et al. [5] and (y1, y2, y3) Binetti et al. [6]. The samples (a), (b) and (c) were annealed in air for 20 hours.

For Si substrate the temperature dependence of PL peak at around 0.8 eV showed a complicated dependence on temperature. But in the cases where SE was applied to substrate, the PL

characteristics changed drastically and the position of the peak shifted to lower energy. Interestingly, the temperature dependence for  $\beta$ -FeSi<sub>2</sub> / Si, SE-treated Si and data for bands of D1 line reported by Binetti et al. [6] appeared to be similar, and the peak energy was located at higher energy than those reported in ref. [5], which is considered as an intrinsic peak of  $\beta$ -FeSi<sub>2</sub>. On the other hand, Fig. 5 compares the temperature dependence of the PL intensity of the samples shown in Fig. 4. The temperature dependence for  $\beta$ -FeSi<sub>2</sub> / Si was similar to that reported in the literature [5], while it appeared to quench at slightly lower temperature than SE-treated Si.

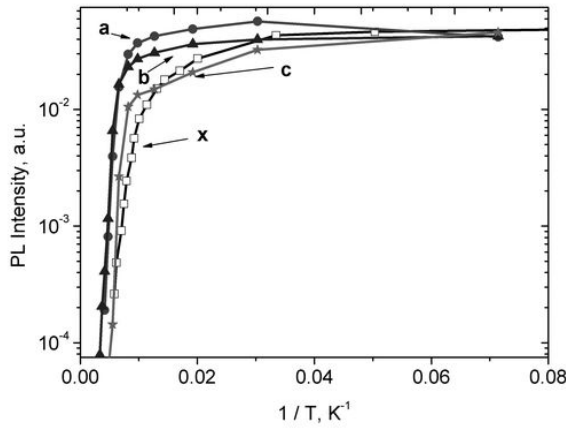


Fig. 5: Temperature dependence of the PL intensity of the samples shown in Fig. 4

The quenching processes shown in Fig. 5 were analyzed, which takes into account two non-radiative processes as shown by the following equation:

$$I(T) = I_0 / [1 + C_1 \exp(\tilde{E}_1 / kT) + C_2 \exp(\tilde{E}_2 / kT)],$$

where  $C_{1,2}$  are the constants for first and second non-radiative processes,  $E_{1,2}$  the activation energies for these processes,  $I_0$  the intensity at  $T = 0$  K and  $k$  the Boltzmann constant. Using this equation the activation energies;  $E_1 = 4$  meV and  $E_2 = 70$  meV,

and the dimensionless constants;  $C_1 = 2.4$  and  $C_2 = 9.8 \times 10^3$ , which correspond to the number density of non-radiative centers, were obtained for the  $\beta$ -FeSi<sub>2</sub> / Si sample after 20 hours of annealing (curve *c*), whereas  $E_1 = 9$  meV,  $C_1 = 2$  and  $E_2 = 116$  meV,  $C_2 = 4 \times 10^4$  were obtained for the annealed Si (SE-treated) (curve *b*). However, the fact the observed peak energy in this study was higher than the literature data indicates that it is unlikely to originate from the intrinsic band of  $\beta$ -FeSi<sub>2</sub>.

#### 4. In search of intrinsic photoluminescence from $\beta$ -FeSi<sub>2</sub>.

##### 4.1 PL from $\beta$ -FeSi<sub>2</sub> formed on SOI substrates.

A substrate with SOI structure is widely applied in semiconductor industry because of its benefit for low power consumption. As a substrate, so-called SIMOX (Silicon IMplanted by OXigen) was employed, where a thin (approximately 100nm) overlayer is situated on insulating BOX (Buried OXide) layer of 100-150 nm in thickness. These samples were thermally annealed in a low vacuum ( $10^{-4}$  Pa) furnace at 1123 K for 24 h, and then PL measurements are carried out. The results are illustrated in Fig. 6.

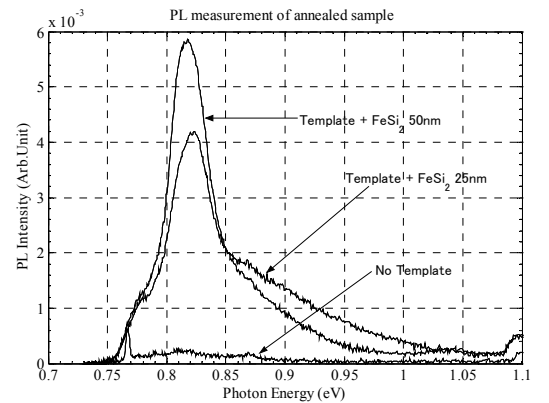


Fig. 6: The PL spectra of annealed  $\beta$ -FeSi<sub>2</sub> sample fabricated without template, with template + 25 nm FeSi<sub>2</sub> deposition and with template + 50 nm FeSi<sub>2</sub> deposition.

The effect of the thermal annealing on the sample without the template (fabricated by deposition of Fe with the approximate thickness of 50 nm) is to quench the 0.82 eV peak. For this sample, the XPS (X-ray photoelectron spectroscopy) analysis and the TEM (transmission electron microscopy) observation showed that the  $\beta$ -FeSi<sub>2</sub> film was considerably aggregated into smaller particles with the size of 20-30 nm. In addition, the interface of the  $\beta$ -FeSi<sub>2</sub> and Si is disappeared where the particles were directly placed on the buried oxide (BOX) layer. On the other hand, it is seen that the film fabricated with the template shows the enhancement of the PL peak intensity at 0.82 eV after annealing. Whereas for the sample without the template, aggregation due to annealing produces the small particles directly placed on the BOX layer. From the temperature dependence of the photoluminescence peak energy and intensity it can be concluded that the PL origin can be same as for the SE Si case from the previous section.

It is deduced that employing template method in fabrication of  $\beta$ -FeSi<sub>2</sub> films on a SIMOX substrate shows the favorable advantage to enhance the PL intensity.

#### 4.2 PL from $\beta$ -FeSi<sub>2</sub> formed on bulk crystal.

It is still unclear from the previous section whether the observed PL signal originated from the  $\beta$ -FeSi<sub>2</sub> or from some other sources. In this section, the PL signal from  $\beta$ -FeSi<sub>2</sub> film, which was grown by molecular beam epitaxy (MBE) on  $\beta$ -FeSi<sub>2</sub> substrate. The  $\beta$ -FeSi<sub>2</sub> substrate was an ingot grown from Ga solvent. The surface of substrates was polished then wet-etched to make it smooth. The PL signal from these samples was measured using the same equipment described

before. The PL intensity was found to be very weak, below the detection limit of the PL measurements. One of possibilities of such weak signal can be attributed to some impurities in this substrate and/or film during preparation process.

### 5. The dependence of PL characteristics on SE energy to Si substrate.

In this section, how the irradiation effect on Si substrate affects the PL properties of  $\beta$ -FeSi<sub>2</sub> film on it. In Fig. 7 the PL spectra of annealed  $\beta$ -FeSi<sub>2</sub> samples fabricated with different incident SE energies are compared.

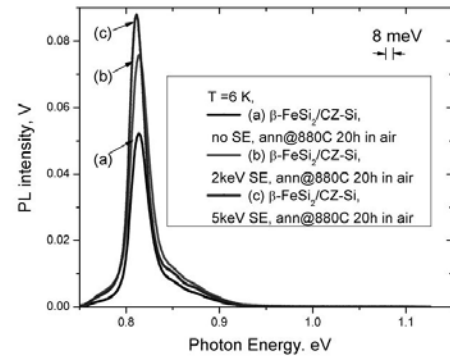


Fig. 7: The PL spectra of annealed samples fabricated with different sputter etching beam energy.

The PL intensity of the annealed  $\beta$ -FeSi<sub>2</sub> on Si substrate increased as the SE energy applied to the substrate increased, thereby indicating the contribution of irradiation defects to the observed PL spectra. Evidence of “critical” sputter etching energy located near of 3 keV sputter etching energy value was found. If the energy of SE ion beam was higher than this “critical” energy the impact of Si related PL in resulting signal is highest. Therefore, Fig. 7 may indicate that SE can be employed to control the PL properties of  $\beta$ -FeSi<sub>2</sub> film on Si substrate.

## Conclusions.

1. A strong photoluminescence peak at around 0.8 eV was observed for  $\beta$ -FeSi<sub>2</sub> films deposited on Si substrates that were sputter etched by Ne<sup>+</sup>, and then thermally annealed in air at elevated temperature. It was revealed that the PL peak at 0.8 eV observed in this study was mainly from D1 emission bands in Si substrate.
2. The  $\beta$ -FeSi<sub>2</sub> films were successfully grown on a thin (100 nm) Si over-layer of SOI substrate by IBSD method, and the  $\beta$ -FeSi<sub>2</sub> was grown on  $\beta$ -FeSi<sub>2</sub> substrate, in order to exclude the contribution of Si substrate to the PL characteristics. It was found that the PL intensity was at least an order of magnitude small than the case when Si substrate was employed.
3. The PL intensity of the annealed  $\beta$ -FeSi<sub>2</sub> on Si substrate increased as the SE energy applied to the substrate increased, thereby indicating the contribution of irradiation defects to the observed PL spectra. Evidence of “critical” sputter etching energy located near of 3 keV sputter etching energy value was found. If the energy of SE ion beam was higher than this “critical” energy the impact of Si related PL in resulting signal is highest.

## 7. References.

- [1] Y. Maeda, K.P. Homewood, T. Suemasu, T. Sadoh, H. Udono, K. Yamaguchi (eds): Thin Solid Films 461, Issue 1, (2004)
- [2] M. Sasase, T. Nakanoya, H. Yamamoto, K. Hojou, Thin Solid Films 401 (2001) 73.
- [3] K. Shimura, T. Katsumata, K. Yamaguchi, H. Yamamoto, K. Hojou, Thin Solid Films 461 (2004) 22.

- [4] K. Yamaguchi, A. Heya, K. Shimura, T. Katsumata, H. Yamamoto, K. Hojou, Thin Solid Films 461 (2004) 17.
- [5] Y. Maeda, Y. Terai, M. Itakura, N. Kuwano, Thin Solid Films 461 (2004) 160.
- [6] S. Binetti, S. Pizzini, E. Leoni, R. Somaschini, A. Castaldini and A. Cavallini, J. Appl. Phys. 92 (2002) 2437.